



Cite this: *Environ. Sci.: Processes Impacts*, 2025, 27, 1054

# Characterizing the distribution of aromatic amines between polyester, cotton, and wool textiles and air†

Özge Edebali,<sup>ID</sup><sup>a</sup> Anna Goellner,<sup>ID</sup><sup>b</sup> Marek Stiborek,<sup>ID</sup><sup>a</sup> Zdeněk Šimek,<sup>a</sup> Melis Muz,<sup>ID</sup><sup>b</sup> Branislav Vrana,<sup>ID</sup><sup>a</sup> and Lisa Melymuk,<sup>ID</sup><sup>\*a</sup>

Textiles play an important role in the accumulation of harmful chemicals and can serve as a secondary source of chemical pollutants in indoor environments, releasing these chemicals back into indoor air, as well as a vector from which indoor pollution can be released by laundering to wastewater systems. Among harmful indoor pollutants, aromatic amines (AAs) are particularly concerning due to their mutagenic and carcinogenic properties, but have received limited attention in non-occupational indoor environments. We have characterized the distribution of 19 AAs between cotton, wool, and polyester textiles and air. Chamber exposure experiments were conducted under controlled laboratory conditions to quantify textile–air distributions of AAs and identify key parameters impacting the distribution. The mass-normalized textile/air distribution coefficients ( $K_{TA}$ ) of AAs for polyester, cotton, and wool range from 5.28 to 9.52 log units ( $L\ kg^{-1}$ ). The findings suggest that cotton generally exhibits higher distribution coefficients than polyester and wool for most analytes. Overall, the results show a strong positive relationship between octanol–air distribution coefficients ( $K_{OA}$ ) and  $K_{TA}$  values. The consistent uptake capacity of all tested textiles for AAs highlights the potential for textiles to play a key role in AA indoor distributions.

Received 7th January 2025  
Accepted 13th March 2025

DOI: 10.1039/d5em00015g  
rsc.li/espi

## Environmental significance

Aromatic amines (AAs) are chemicals of concern due to their mutagenic and carcinogenic properties. Understanding their sources is essential to reduce environmental levels. Textiles play a key role in indoor environments as they can act as sinks for semi-volatile compounds and a transport medium to outdoors via laundering. We quantify the distribution coefficients of AAs between different types of textiles and air, which can help understand the importance of textiles in human exposure to AAs and in their transport from indoor to outdoor environments.

## 1 Introduction

Textile surfaces are common elements in indoor environments, covering large surface areas in the form of upholstery, curtains, carpets, and clothing.<sup>1</sup> These textile surfaces can act as significant reservoirs of various harmful chemicals.<sup>2</sup> Given that people spend most of their time indoors, the role of textiles as potential emitters or absorbers of those chemicals is particularly important.<sup>3,4</sup>

Textile structure and chemical properties influence their sorptive capacities.<sup>5,6</sup> Textile fibres can be classified as natural (e.g., cotton and wool), semisynthetic (e.g., rayon), and synthetic (e.g., polyester) materials. Cotton and wool fibres have large,

irregular surfaces and a porous structure. Synthetic fibres like polyester have smoother, more uniform surfaces.<sup>4</sup> The sorption behaviour varies with fabric type, with natural fibres generally having a higher affinity for polar semi-volatile organic compounds than nonpolar synthetic fibres.<sup>6,7</sup> For example, natural textiles absorb more cigarette smoke and gain significantly more weight than synthetic materials like polyester primarily due to the particulates in the smoke.<sup>8,9</sup> Noble<sup>5</sup> measured the change in textile weight during exposure to cigarette smoke, finding the greatest weight gain for rayon, linen, wool, and cotton, while polyester gained the least. Cotton, for example, absorbed about ten times more smoke than polyester. Smoke absorption and moisture regain are correlated, with fabrics that absorb more moisture also tending to absorb more smoke.<sup>5</sup> Differences in the surface area-normalized sorption of polybrominated diphenyl ethers to cotton and polyester were attributed to both micro-surface differences in textile properties and differences in chemical affinity due to textile compositions.<sup>10</sup>

Textiles have been shown to be key matrices impacting secondary emissions of chemicals back to the indoor

<sup>a</sup>RECETOX, Faculty of Science, Masaryk University, Kotlarska 2, 61137 Brno, Czech Republic. E-mail: lisa.melymuk@recetox.muni.cz

<sup>b</sup>UFZ Helmholtz Centre for Environmental Research, Department of Exposure Science, Permoserstr. 15, 04318 Leipzig, Germany

† Electronic supplementary information (ESI) available. See DOI: <https://doi.org/10.1039/d5em00015g>



environment, as well as vectors through which chemicals can be transferred to outdoor environments.<sup>11</sup> For example, nicotine, a major alkaloid in tobacco smoke, rapidly sorbs to surfaces, including clothing, skin, and hair, contributing to third-hand smoke exposure.<sup>12</sup> Won *et al.*<sup>2</sup> found that carpets can absorb and gradually re-emit volatile organic compounds, thereby changing peak indoor air concentrations.

Moreover, recent attention has been given to the transfer of chemicals from indoor environments to outdoor surface waters *via* wastewater discharges<sup>13</sup> and washing of textiles is a key component of this transfer. Saini *et al.*<sup>4</sup> investigated the transfer of phthalates, brominated flame retardants, and organophosphate esters from indoor air to cotton and polyester and subsequent release to water during washing, identifying the importance of laundry discharges in transferring plastic additives from indoor to outdoor environments.

Aromatic amines (AAs) are a broad compound group known to be hazardous to human health and the environment, but in indoor environments largely associated with occupational exposure.<sup>14</sup> They are used in rubber, azo dyes, pesticides, plastics, pharmaceuticals, cosmetics, and textiles, and can be produced in cigarette smoke and by high-temperature cooking of protein-rich foods such as meats and fish.<sup>15–17</sup> Certain AAs are classified as carcinogens or potential carcinogens for humans<sup>18</sup> and are contributors to both acute toxicity<sup>19,20</sup> and mutagenicity in surface waters.<sup>21</sup> There is growing awareness of the potential for these chemicals to be important indoor contaminants in non-industrial indoor environments, including in homes.<sup>14,22</sup> AAs can accumulate in textiles through direct contact with indoor sources such as tobacco smoke, cooking, foods, and hair dyes,<sup>14</sup> as well as through deposition of airborne particles, dust, or contaminated air. Given the importance of indoor textiles in the uptake and release of chemicals from tobacco smoke, which includes AAs, we hypothesize that indoor textiles can play an important role in the distribution of AAs in indoor environments, as well as their release to outdoor environments *via* laundry wastewater. However, little is known about the sorptive behaviour of AAs to textiles, which is necessary to understand their role in the accumulation and retention of these compounds.

This study investigates the sorptive distribution of AAs between three textiles (wool, cotton, and polyester) and air, providing insights into their indoor fate. To determine the

distributions of AAs between textiles and air, we designed a chamber exposure study using primary AAs and three types of textiles. Initial laboratory work focused on developing techniques for dosing and extraction of AAs to textiles. Subsequent laboratory exposure experiments were conducted to determine the textile–air distribution coefficients ( $K_{TA}$ ) of AAs.

## 2 Materials and methods

### 2.1. Determination of textile–air distribution coefficients

The purpose of the experiment was to determine textile–air distribution coefficients of selected AAs (Table S2<sup>†</sup>) under laboratory conditions as a ratio of concentration in the textile fabric and concentration in the adjacent air under equilibrium conditions. The experiment was performed by extracting AAs (by trapping on Tenax® TA sorbent) from a defined volume of air that was in contact with a piece of textile containing a range of AAs inside an exposure chamber. Following each textile's exposure to air, concentrations of AAs in the textile sample were determined after solvent extraction of the textile.

The experimental apparatus consisted of a textile exposure chamber consisting of a three-litre glass cylinder with a flat bottom and a ground-joint flange lid (Fig. 1). The exposure chamber was designed with a threaded air inlet in the lid, implemented as a steel capillary pierced through a septum, and an air outlet at the bottom. The chamber operated in a flow-through setup, meaning it was not a closed system. We assumed that the dosing rate of the textile (in terms of air volume equivalent per unit of time) was significantly higher than the airflow rate. Consequently, the chamber conditions were maintained close to a textile/air distribution equilibrium. A wire mesh sheet was rolled up inside the chamber, serving as a framework to support a piece of the tested textile. A small fan inside the chamber was used to homogenize the air inside the chamber and minimize the air boundary layer at the surface of the textile. The chamber was kept at a constant temperature of 25 °C through an external thermostatic water circuit.

Two glass tubes packed with Tenax® TA (Gerstel, Germany) were connected in series to the chamber outlet to trap AAs from the air extracted from the exposure chamber. Air was drawn from the apparatus through the Tenax tubes using a low-volume air pump connected to a digital air mass flow controller (Omega

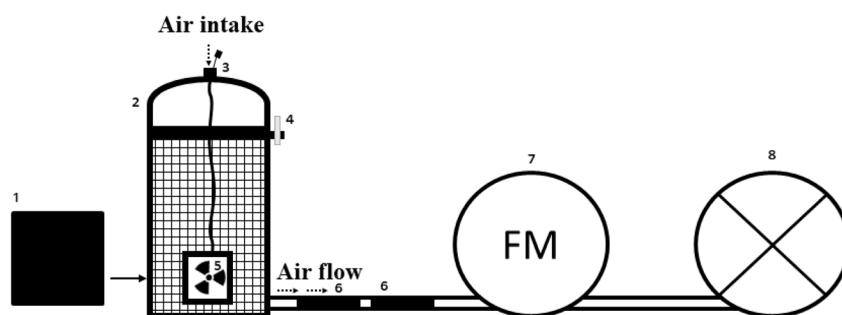


Fig. 1 Scheme of apparatus used for measurement of  $K_{TA}$  of AAs; 1- textile pieces before wrapping to the chamber mesh (Fig S1<sup>†</sup>), 2- glass chamber with a ground joint lid, mesh and airtight seal, 3- steel capillary pierced through a septum for air intake, 4- metal clamp, 5- small fan, 6- two glass tubes filled with Tenax adsorbent, in series, 7- air mass flow meter, 8- low volume air pump.



FMA-A2404, USA) adjustable in the 0–200 standard cubic centimetres per minute (sccm) range.

## 2.2. Textile and Tenax preparation

Tenax tubes (Tenax® TA thermal desorption tubes, 6 × 60 mm, Gerstel, Germany) were pre-cleaned before each experiment with methyl *tert*-butylether (MTBE, 12 h, Soxhlet extraction). After solvent cleaning, tubes were placed into a tube conditioner (Gerstel TC2, Gerstel, Germany) and dried for 2 h in a pure nitrogen stream at 300 °C.

Three types of textile materials were tested: wool, cotton, and polyester. All textiles were white/undyed materials; detailed information is provided in ESI Fig. S2, Text S1 and Table S1.† The purchased textile fabrics were cut into larger sheets (27 × 32 cm; area of 864 cm<sup>2</sup> each), pre-cleaned (cleaned in water in overhead tumbler) and dried (Text S1 and Fig. S3†). Textiles were then dosed with a mixture of 19 primary AA compounds (Table S2†). The dosing procedure in a rotary evaporator was selected after testing different dosing methods to ensure homogeneously dosed textile samples (Text S2 and Fig. S4–S7†). The selected AAs were diluted in acetone by spiking 1 mL of AA standard (for the spiked masses of each analyte see Table S3†) in approximately 200 mL of acetone in a round rotary evaporator flask and mixed by shaking for 5 minutes. Next, the textile sheet was added to the acetone-filled flask. The textile samples were dosed for 6 hours while turning on a rotary evaporator (270 rpm, 25 °C at normal pressure). Subsequently, acetone was evaporated (556 mbar, 40 °C) while continuing the flask rotation, a process taking 1 hour to achieve complete dryness. After dosing, the textile samples were stored in the closed rotary evaporator flask at 4 °C until they were transferred to the exposure chamber.

## 2.3. Chamber test experiment conditions

The AA concentrations applied for dosing the textile sheets (Table S3†), were pre-calculated to ensure a reliable detection of AAs in the air sampled from the exposure chamber, and to confirm a negligible AA depletion (<5% concentration decrease) from the textile material by desorption to air during the experiment. For the pre-calculation, without an *a priori* knowledge of the magnitude of the textile–air distribution coefficient  $K_{TA}$ , it was approximated that it is equal to the octanol–air partition coefficient ( $K_{TA} = K_{OA}$ ). The expected uptake capacity of the textile for AAs was calculated as  $V_{A,max} = K_{TA} \times V_T$ , where  $V_T$  is the volume of the tested textile sheet. The product is the maximum equivalent volume of air ( $V_{A,max}$ ) sampled by partitioning between the air and the textile. The desorption of AA from textile can be considered non-depletive ( $V_{A,nd}$ ) when the sampled air volume is negligibly low in comparison with the uptake capacity, *i.e.* when  $V_{A,nd} \ll V_{A,max}$ ; in our case we considered  $V_{A,nd} \leq 0.05 \times V_{A,max}$ . The volume of air passed through the chamber during the experiment was calculated so that the mass of AA removed by the air flow from the textile did not significantly decrease the AA concentration in the textile during the experiments. With the exception of ANI and OTLD ( $V_{A,nd} \sim 23$  and 62 L), the sampled air volume  $V_{A,nd}$  that should

not cause any significant AA depletion from textile was calculated to be higher than 100 L, ranging from 340 L for 4CHA and  $4 \times 10^{11}$  L for 2A4NT. Based on these estimates, 100 L of sampled air of was set as a constant used in our experimental  $K_{TA}$  measurements. In the next step, the required mass of AA spiked on the textile was calculated, that would result in well detectable amounts of an AA in the sampled 100 L air (>0.1 ng) by equilibrium partitioning from textile. With the exception of some AAs with very high  $K_{OA}$  (33DCB, 2A4NT, MBOCA), spiking 10–100 µg AA on the textile is considered sufficient for their detection in the equilibrated 100 L air sample.

Prepared textiles (27 × 32 cm) were dosed with AAs and pre-cut into 2 cm<sup>2</sup> pieces to ease subsampling of textiles during the chamber experiments with limited disturbance to the experimental setup. Before placing the textile rectangles into the chamber, six subsamples of 2 cm<sup>2</sup> were collected from each piece to assess the dosing homogeneity. Subsequently, the AA-dosed textile piece, wrapped around the wire mesh, was placed into a glass cylindrical chamber. The chamber was closed, and the experiments were initiated. Two durations of experiments were performed: 8-hour and 24-hour exposures. For the 24-hour experiments, triplicate data were collected over three days with a constant airflow of 67 sccm through the chamber. Similarly, the 8-hour experiment was conducted with a higher airflow of 200 sccm, keeping the total sampled air volume constant (96 L). The measurement of AA concentration in the freshly spiked textile samples *versus* textile samples exposed in the chamber confirmed that the sampling did not decrease the AA concentration in the textile by more than 1%. After each experiment, the air pump was stopped, and the Tenax tubes were transferred to separate vials and stored in the freezer for subsequent AA analysis. The chamber was opened, and nine 2 cm<sup>2</sup> textile pieces were removed with tweezers, placed into vials and stored for AA analysis. This procedure was repeated for each textile type, with triplicate experiments conducted for both 24-hour and 8-hour durations.

## 2.4. Extraction of aromatic amines

**2.4.1 Textile extraction.** The method for textile extraction was selected after testing three solvent options (Text S3 and Fig. S8†); the selected method used MTBE as the extraction solvent. Textile samples (2 cm<sup>2</sup>) were placed in 15 mL amber glass vials. Surrogate standards (Section 2.6) and 5 mL of MTBE were added to each vial, and the samples were subjected to ultrasonication for 15 minutes. The extract was transferred to the Syncore evaporator flasks (Büchi Labortechnik AG, Switzerland; 250 mL). This extraction step was repeated to maximize analyte recovery. The combined extracts were transferred to Syncore glass flasks and then reduced in volume using a multi-position Büchi Syncore analyst rotary evaporator (Büchi Labortechnik AG, Switzerland) to approximately 0.5 mL (185 mBar, 60–65 °C). The final extracts were solvent exchanged by adding the target solvent acetonitrile (ACN, 99.95%, Biosolve, Netherlands) to the flask and concentrated to 1 mL. The concentrated extract was subsequently filtered to remove any remaining particles with a nylon syringe filter (Chromafil Xtra PA-20/13,



pore size 0.20  $\mu\text{m}$ , diameter 13 mm, Macherey-Nagel, Germany) into clean LC autosampler vials.

**2.4.2 Extraction of AAs from Tenax (gas phase samples).** Surrogate standards (see Section 2.6) were added to the samples (sorbent inside the Tenax tube), and the AAs were then eluted from Tenax tubes with 5 mL of ACN. Following elution, the solvent volume was reduced to 1 mL using a nitrogen stream. A similar filtration procedure as described for the textiles was applied to the gas phase extracts.

## 2.5. Analysis

The chromatographic separation of target compounds in the textile and Tenax extracts was performed using a liquid chromatograph (Agilent 1290 II LC System, Agilent Technologies, Santa Clara, CA) equipped with a Kinetex F5 Core-Shell HPLC Column and a precolumn (150  $\times$  2.1 mm, 1.7  $\mu\text{m}$  particle size, Phenomenex, Torrance, CA). Extracts and calibration solutions of the standard mixture, prepared in the concentration range of 1.0–250  $\text{ng mL}^{-1}$  in ACN, were diluted, mixed, and injected using a sandwich injection technique. The injection sequence consisted of 3  $\mu\text{L}$  of distilled water, followed by 1  $\mu\text{L}$  of the sample or calibration solution, 0.5  $\mu\text{L}$  of an internal deuterated standard mixture in ACN, and another 3  $\mu\text{L}$  of distilled water. The final composition of the injected sample or calibration solution was 80% water and 20% ACN. Five deuterated AAs, used as internal standards (ISTD) at a concentration of 50  $\text{ng mL}^{-1}$ , were selected to span the retention time range of the target amine mixture. The column temperature was set to 35  $^{\circ}\text{C}$ . The mobile phase consisted of water (A) and ACN/methanol (50/50) (B), both containing 0.1% (v/v) formic acid. The gradient program was as follows: 0 min, 10% B; 0–7 min, increased from 10% to 98% B; 7–10 min, held at 98% B; 10–10.3 min, decreased from 98% to 10% B, followed by a re-equilibration at 10% B until 20 min. The flow rate was maintained at 0.3  $\text{mL min}^{-1}$ .

An Agilent 6495A Triple Quadrupole Mass Spectrometer (Agilent Technologies, Santa Clara, CA) with a mass resolution of 0.7 amu (FWHM, autotune) and mass accuracy of 0.1 amu from 5 to 1000  $m/z$  was used to quantify AAs. The ion source parameters were set as follows: gas temperature of 280  $^{\circ}\text{C}$ , gas flow at 15  $\text{L min}^{-1}$ , nebulizer pressure at 25 psi, sheath gas temperature at 380  $^{\circ}\text{C}$ , sheath gas flow at 12  $\text{L min}^{-1}$ , capillary voltage of 3000 V (positive mode), and nozzle voltage of 300 V. The instrument operated in ESI-positive dynamic multiple reaction monitoring (dMRM) mode. For MS/MS analysis, two transitions were monitored for each analyte. Collision energies for the  $[\text{M} + \text{H}]^+$  precursor ions of both target analytes and ISTDs are provided in Table S4.† Agilent MassHunter Workstation Software, LC/MS Data Acquisition (version B.08.00) for the 6400 Series Triple Quadrupole, was used for dMRM data acquisition, while AA quantification was performed using Agilent MassHunter Quantitative Analysis software, version B.07.01 for QQQ.

## 2.6. QA/QC

The extraction efficiency of AAs from Tenax tubes was tested by spiking Tenax tubes with a mixture of primary AAs ( $n = 3$ ), with recoveries averaging  $100 \pm 25\%$  (Fig. S9†). The potential for

analyte breakthrough was assessed by connecting a second Tenax tube in series, and no quantifiable AAs were present, indicating no breakthrough (Table S5†). The extraction efficiency of AAs from textiles was evaluated through spiking tests ( $n = 3$  per textile type), averaging  $61 \pm 14\%$  for polyester,  $53 \pm 17\%$  for cotton, and  $71 \pm 26\%$  for wool (Fig. S7†).

Surrogate standards  $d_8$ -benzidine (Dr Ehrenstorfer™, LGC Group, USA) and  $d_3$ -*o*-anisidine (A2S Analytical Standard Solutions, France), 100 ng per sample, were added to each sample before extraction to monitor the recoveries of AAs. Surrogate recoveries ranged from 65% to 87% for textile samples and from 81% to 118% for Tenax tubes (Tables S6 and S7†). Laboratory blanks (3 samples from each pre-cleaned textile material) were spiked with surrogate standards, and target AAs were below detection limits in all blanks.

## 2.7. Calculation of $K_{\text{TA}}$ and associated uncertainties

Each series of experiments resulted in six sets of paired air and textile data (*i.e.*, three replicates with 8 h duration and three replicates at 24 h air sampling duration). For each set, nine textile subsamples and one Tenax sample for gas phase analysis were evaluated.

Each textile subsample was weighed. The nine AA concentrations in textile subsamples were averaged for each replicated experiment. The textile/air distribution coefficient of each AA in each experiment,  $K_{\text{TA}}$  ( $\text{L kg}^{-1}$ ), was calculated as the ratio:

$$K_{\text{TA}} = \frac{N_{\text{T}} V_{\text{A}}}{N_{\text{A}} m_{\text{T}}} \quad (1)$$

where  $N_{\text{T}}$  is the average mass of an AA extracted from the textile subsamples ( $n = 9$ ),  $m_{\text{T}}$  is the average mass of the textile sample ( $n = 9$ ),  $N_{\text{A}}$  is the mass of an AA extracted from the Tenax sample ( $n = 1$ ) and  $V_{\text{A}}$  is the volume of sampled air ( $V_{\text{A}} = 96 \text{ L}$ ).

Uncertainties in  $K_{\text{TA}}$  values were also estimated (Text S3†). Since only one Tenax sample was used per experiment, the uncertainty in the air concentrations was calculated by incorporating sources of uncertainty in the measurement: the error from the flow controller, repeatability of Tenax analysis, and extraction recoveries of AA from Tenax. For textiles, the standard deviation of the nine textile subsamples was taken to indicate uncertainty. Calculated  $K_{\text{TA}}$  values were compared across replicates and exposure durations (one-way ANOVA test;  $\alpha = 0.05$ ) to determine if the differences in the mean  $K_{\text{TA}}$  values were statistically significant.

We also evaluated literature values for volume normalized textile–air distribution coefficient ( $K_{\text{vol}}$ ) in comparison with the  $\log K_{\text{OA}} - \log K_{\text{vol}}$  relationship we obtained, using cotton fabrics as a comparison as cotton had the best data availability. We calculated volume-normalized data from our mass-normalized distribution coefficients data (Table S8†). The volume-normalized cloth–air partition ratio,  $K_{\text{vol}}$ , was calculated as:

$$K_{\text{vol}} = K_{\text{TA}} \times \rho_{\text{T}} \quad (2)$$

where  $K_{\text{vol}}$  is unitless, *i.e.* ( $\text{L kg}^{-1}$ )  $\times$  ( $\text{kg L}^{-1}$ );  $K_{\text{TA}}$  textile–air distribution coefficient ( $\text{L kg}^{-1}$ ) and  $\rho_{\text{T}}$  ( $\text{g cm}^{-3}$ ) is textile density given in Table S1.†



### 3 Results and discussion

#### 3.1. Determination of textile–air distribution coefficients ( $K_{TA}$ )

The measurement was successfully conducted for 19 AAs, with values obtained for all three tested materials. Table 1 provides the average  $\log K_{TA}$  for AAs in polyester, cotton, and wool.  $K_{TA}$  values were not determined for OAAT, PAAZB, ODAN and MBOCA in wool and PAAZB for cotton due to their high  $K_{OA}$  (and corresponding  $K_{TA}$ ) values, which led to air concentrations below the instrumental limit of quantification (LOQ). The spiked concentrations of these compounds on the textiles were likely too low to produce detectable air levels.

For polyester textiles, the ANOVA results (Table S9†) indicated no significant difference between the three replicates within 8-hour and 24-hour experiments. The airflow did not significantly affect the measured  $K_{TA}$ , indicating that textile/air equilibrium was consistently achieved for all compounds under both 8- and 24-hour conditions, thereby confirming that the experimental setup provided sufficient time for equilibrium to be established regardless of the airflow rate. Consequently, the  $K_{TA}$  data for polyester textiles were averaged (Fig. 2A) across all experiments. For cotton and wool textiles, the ANOVA results (Table S9†) showed a significant difference between the first replicate and subsequent replicates, but no significant difference between the second and third replicates. Therefore, the data for the 24-hour and 8-hour experiments were averaged for these textile types, excluding the first replicates (Fig. 2B, and C). We hypothesize that the chamber system had not achieved equilibrium at the time of collection of the first replicates for wool and cotton, which may have been due to some solvent (acetone) retention in cotton and wool. Both fabrics have higher capacities for retaining liquid and it is possible that some

solvent from AA spiking was retained in the textile, and subsequently evaporated into the chamber air and disturbed the equilibrium conditions. As a result, the data from the first replicates for cotton and wool were excluded.

#### 3.2. Factors affecting textile–air distributions

All textile types had a substantive sorptive capacity for AAs, with clear positive relationships between  $\log K_{TA}$  and  $\log K_{OA}$  (Fig. 3).

$$\log K_{\text{polyester-air}} = 0.73 \log K_{OA} + 1.5, r^2 = 0.61, n = 19, SE = 0.14 \quad (3)$$

$$\log K_{\text{wool-air}} = 0.54 \log K_{OA} + 2.8, r^2 = 0.60, n = 15, SE = 0.12 \quad (4)$$

$$\log K_{\text{cotton-air}} = 0.78 \log K_{OA} + 1.4, r^2 = 0.60, n = 18, SE = 0.17 \quad (5)$$

The correlations obtained for these empirical relationships suggest that they may be used to interpolate the prediction of textile–air distribution for other structurally similar compounds, e.g., other primary AAs based on regression eqn (3)–(5).

For compounds with  $\log K_{OA}$  above 8, cotton shows higher  $\log K_{TA}$  values than wool or polyester, indicating a high capacity to sorb AAs. The higher sorptive capacity of cotton in comparison with the other two textile materials aligns with what has been noted by Borujeni *et al.*,<sup>8</sup> who also identified that cotton had a high capacity to adsorb tobacco smoke compounds such as pyridine and nicotine, and those of Morrison *et al.*,<sup>3</sup> who noted that cotton exhibited higher  $\log K_{TA}$  for methamphetamine than polyester. Similar to our observations, Saini *et al.*<sup>4</sup> found that cotton fabrics had higher partition coefficients than

**Table 1** Measured textile/air distribution coefficients  $K_{TA}$  ( $L \text{ kg}^{-1}$ ).  $K_{OA}$  data were obtained from the Comptox dashboard<sup>a23,24</sup>

Compound name	Abbr	Log $K_{OA}$	Polyester $\log K_{TA} \pm$ standard dev	Wool $\log K_{TA} \pm$ standard dev	Cotton $\log K_{TA} \pm$ standard dev
Aniline	ANI	4.94	5.28 ± 0.21	5.46 ± 0.20	5.53 ± 0.12
2-Aminopyridine	2APY	5.68	6.07 ± 0.13	6.44 ± 0.19	6.81 ± 0.23
<i>o</i> -Toluidine	OTLD	5.91	5.36 ± 0.20	5.50 ± 0.20	5.48 ± 0.17
<i>o</i> -Anisidine	OANI	6.15	5.91 ± 0.32	6.03 ± 0.20	6.14 ± 0.15
4-Chloroaniline	4CHA	6.25	6.18 ± 0.16	6.31 ± 0.21	6.13 ± 0.13
<i>p</i> -Cresidine	PCRE	7.28	6.45 ± 0.28	6.31 ± 0.19	6.47 ± 0.17
3-Chloro- <i>o</i> -Toluidine	3CHOT	7.46	5.94 ± 0.16	6.03 ± 0.18	6.02 ± 0.11
4-Chloro- <i>o</i> -Toluidine	4CHOT	7.48	6.25 ± 0.16	6.26 ± 0.20	6.19 ± 0.12
2-Amino-4-nitrotoluene	2A4NT	7.59	7.97 ± 0.15	7.81 ± 0.29	8.07 ± 0.16
Benzidine	BNZD	8.35	8.16 ± 0.72	8.58 ± 0.40	9.29 ± 0.16
<i>o</i> -Aminoazotoluene	OAAT	8.46	9.22 ± 0.20	—	9.55 ± 0.19 <sup>b</sup>
1-Naphthylamine	1NAPA	8.47	7.58 ± 0.30	7.28 ± 0.25	7.39 ± 0.20
2-Naphthylamine	2NAPA	8.47	7.45 ± 0.31	7.59 ± 0.27	7.67 ± 0.22
<i>p</i> -Aminoazobenzene	PAAZB	8.70	8.85 ± 0.24	—	—
3,3'-Dichlorobenzidine	33DCB	9.11	7.81 ± 0.40	8.00 ± 0.38	8.31 ± 0.14
<i>o</i> -Dianisidine	ODAN	9.11	7.50 ± 0.16	—	9.51 ± 0.10 <sup>b</sup>
4,4'-Methylenebis(2-chloroaniline)	MBOCA	9.15	9.52 ± 0.29	—	9.65 ± 0.14 <sup>b</sup>
2-Aminobiphenyl	2AMB	9.27	6.72 ± 0.16	6.79 ± 0.19	6.84 ± 0.12
4-Aminobiphenyl	4AMB	9.27	8.17 ± 0.19	7.91 ± 0.29	8.25 ± 0.14

<sup>a</sup> —: Indicates that air concentration data was unavailable, preventing the calculation of  $K_{TA}$  values. <sup>b</sup> AAs were quantified in only 18 out of 36 samples; samples <LOQ were not considered in the calculation.



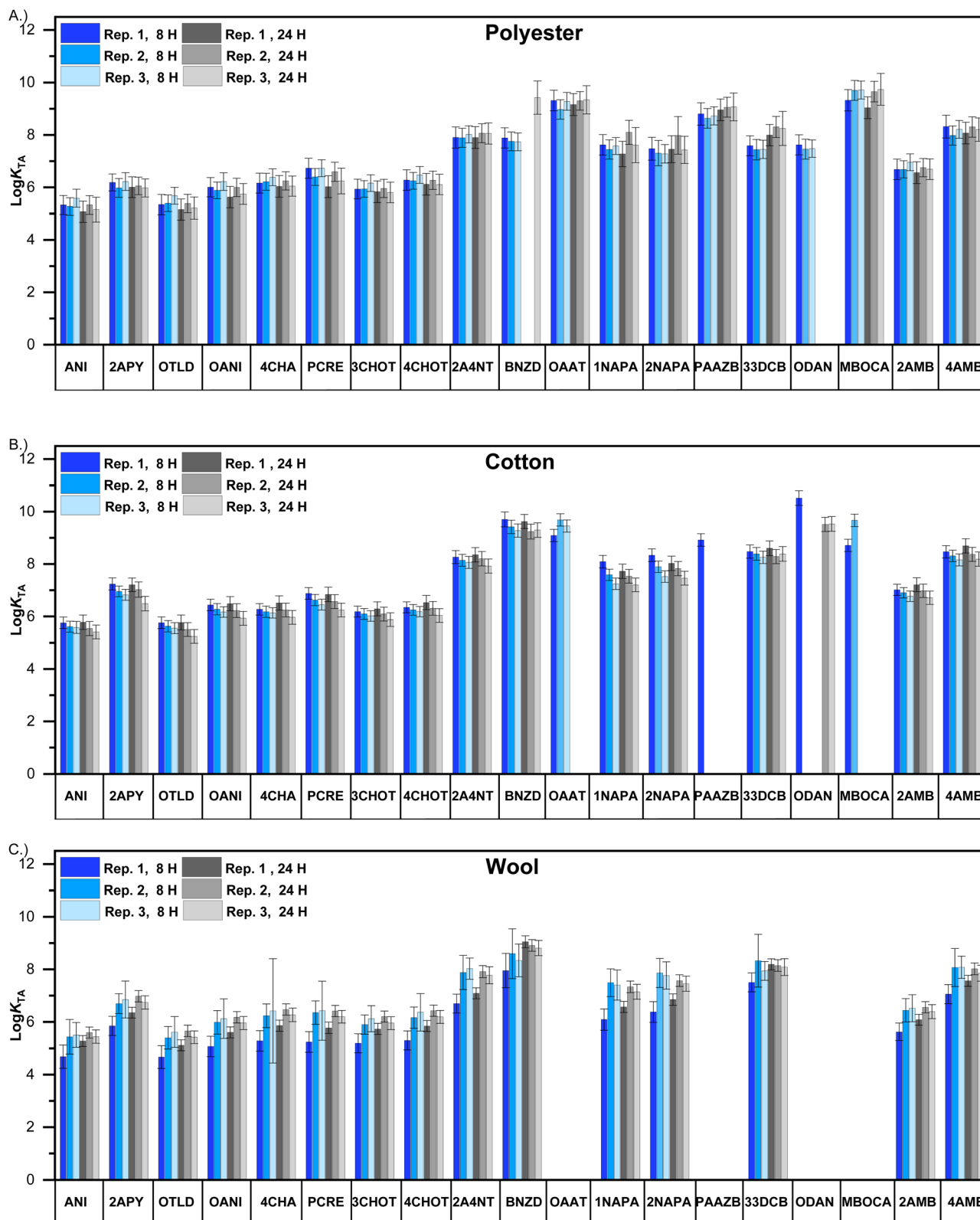


Fig. 2  $K_{TA}$  ( $L\ kg^{-1}$ , log-transformed) of aromatic amines for three types of textiles — (A) polyester, (B) cotton, and (C) wool. Data were collected from two experiments performed at two different air flow conditions (thus differing in experiment duration of 8 hours and 24 hours); each experiment was conducted in triplicate.



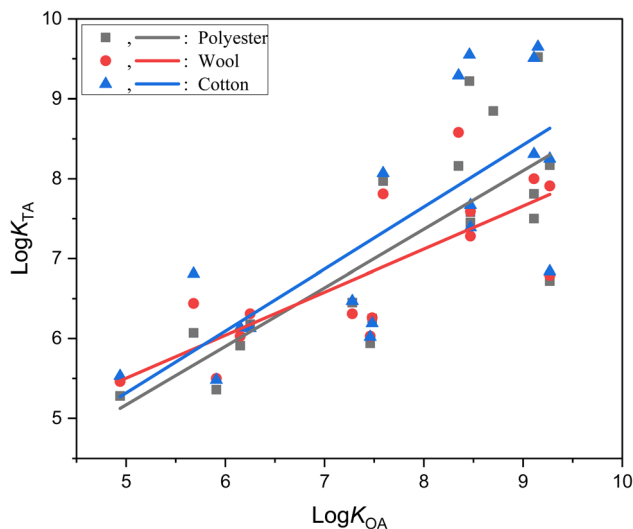


Fig. 3 Linear regression of  $\log K_{TA}$  as dependent on  $\log K_{OA}$ .

rayon for semi-volatile organic compounds (SVOCs), reinforcing the pattern that cotton consistently shows higher retention of chemicals across various studies. Fibres are often classified based on their origins into two main categories: natural fibres and synthetic fibres, which are derived from natural or synthetic polymers.<sup>25</sup> Cotton, as a natural fibre, is hydrophilic due to its structure rich in hydroxyl groups that strongly attract and absorb water molecules.<sup>25,26</sup> This high moisture absorbance increases cotton's ability to absorb airborne chemicals, especially polar molecules.<sup>12</sup> The higher  $K_{TA}$  observed for cotton textiles in our study, as well as in other studies, may be due to the hydrophilic nature of the textile fibres. In contrast, polyester is hydrophobic,<sup>27</sup> with a smooth surface and a chemical structure that repels water, reducing its capacity to adsorb chemicals from the air. This limited adsorption might give polyester a lower capacity than cotton to interact with airborne chemicals. These contrasting properties are critical for understanding chemical interactions with textiles.

Further, even with the overall correlation with  $\log K_{OA}$ , individual AAs showed variations in  $\log K_{TA}$  values across textiles, suggesting that the affinity of AAs can vary depending on the textile material-compound property combination. A few compounds had  $K_{TA}$  values that were consistently more than one order of magnitude lower than the corresponding  $K_{OA}$ . A notable example is 2AMB, with  $\log K_{TA}$  values of  $\sim 6.8$  compared with  $\log K_{OA}$  of 9.27; in contrast, 4AMB, which differs only in the position of the amino group, had  $\log K_{TA}$  values of 7.9–8.2 (Table 1). This suggests weaker interactions of 2AMB with all textiles. 2AMB (*ortho*) and 4AMB (*para*) differ in chemical hydrogen bonding,<sup>28</sup> and key structural characteristics that might influence their behaviour. In contrast, OAAT and MBOCA (for polyester and cotton) and BNZD (for cotton only) exhibited  $K_{TA}$  values that were substantially higher than  $K_{OA}$  (Table 1), indicating greater affinity for textiles than for pure organic matrices.

The literature has limited data on partitioning measurements between fabrics and air, making direct comparisons of

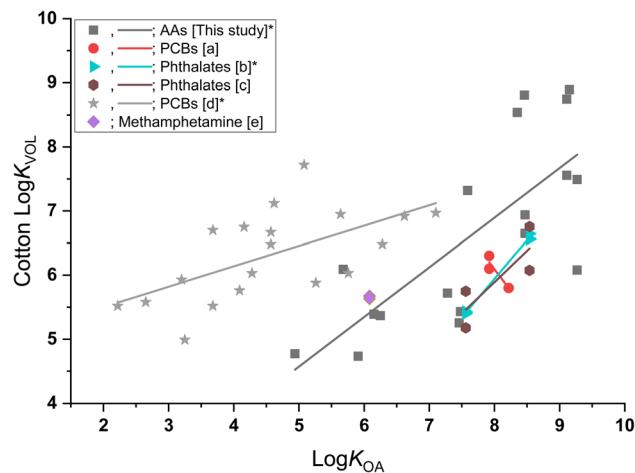


Fig. 4 Cotton textile  $K_{vol}$  for different compounds from literature; AAs (this study), PCBs [a],<sup>29</sup> phthalates [b],<sup>32</sup> phthalates [c],<sup>31</sup> PCBs [d],<sup>30</sup> methamphetamine [e].<sup>3</sup> The regressions marked with an asterisk (\*) indicate that at the 0.05 level, the slope is significantly different from zero. The statistical values for the linear regression analysis are provided in Table S10.†

the same compounds challenging. However, existing studies provide ranges for SVOCs such as novel flame retardants (NFRs) and phthalates, showing some consistency in partitioning behaviour across different compound groups. Other studies have linked fabric-air distribution to physical-chemical compound properties such as  $K_{OA}$ , including for methamphetamine,<sup>3</sup> PCBs,<sup>29,30</sup> and phthalates.<sup>31,32</sup> Morrison *et al.*<sup>32</sup> also investigated textile-air partition coefficients for diethyl phthalate and di-*n*-butyl phthalate using a closed chamber experiment over 10 days. They observed that fabric-air partition coefficients of phthalates were strongly linked to  $K_{OA}$  values, a trend also evident in our findings for AAs. Additionally, Saini *et al.*<sup>4,10</sup> reported area normalized distribution coefficients for cotton and rayon fabrics for NFRs, PBDEs, and phthalates, showing that the distribution of chemicals was positively correlated with  $K_{OA}$ , and consistent with the kinetic limitations of uptake.

The  $K_{TA}$  values for AAs, phthalates,<sup>32</sup> and PCBs<sup>30</sup> showed strong positive relationships between  $\log K_{OA}$ – $\log K_{vol}$ , as in our AA data (Fig. 4 and Table S10†). Variations in experimental design, including environmental conditions and fabric structure likely contribute to the differences in partition ratios and equilibration times observed in these studies. Additionally, differences in extraction methods may further contribute to these differences, even for the same chemicals.

## 4 Limitations

Our study only included one representative fabric from each fabric type (cotton, wool, and polyester). Previous research has shown that variations within the same fabric type, such as differences in cotton varieties, can affect air-fabric distributions,<sup>30</sup> therefore expanding the number of textile samples in future studies would provide a more comprehensive



understanding of their impact. Additionally, while the moisture content of the fabric was not determined in this study, studies have shown that natural and synthetic fibres have different moisture regain capacities.<sup>5</sup> While some literature provides data on textile moisture content,<sup>4,33</sup> direct measurements in our study would have allowed for a clearer understanding of how moisture levels affect the distribution of AAs.

## 5 Conclusions

Chamber studies were conducted to determine the distribution coefficients between the concentrations of AAs in air and their sorption by polyester, cotton, and wool textiles. The results indicate that cotton generally exhibits higher distribution coefficients compared to polyester and wool for most analytes. A positive correlation was observed between the  $K_{TA}$  values and the  $K_{OA}$ . Empirical equations can be employed to estimate distribution for other structurally similar compounds from the aromatic amine compound class. Further, understanding the indoor exposure potential of AAs *via* textiles will provide insights into their behaviour across different fabric types.

## Data availability

Data supporting this article have been included as part of the ESI.† Additional primary experimental data (measured concentrations of AAs in textiles and air used to calculate distribution coefficients) are available at [zenodo.org](https://zenodo.org/10.5281/zenodo.14608630) at <https://doi.org/10.5281/zenodo.14608630>.

## Author contributions

OE: Methodology, investigation, visualization, formal analysis, writing – original draft; AG: methodology, writing – review & editing; MS: methodology, investigation, writing – review & editing; ZS: methodology, investigation, writing – review & editing; MM: conceptualization, writing – review & editing; BV: methodology, conceptualization, supervision, writing – review & editing; LM: formal analysis, supervision, writing – review & editing.

## Conflicts of interest

There are no conflicts to declare.

## Acknowledgements

The project results were created with the financial support of the provider Czech Science Foundation within the project no. GF22-06020K and Deutsche Forschungsgemeinschaft (DFG, German Research Foundation) – MU 4728/2-1. The authors thank the RECETOX Research Infrastructure (LM2023069) financed by The Ministry of Education, Youth and Sports for a supportive background. This work was supported from the European Union's Horizon 2020 research and innovation program under grant agreement no. 857560 (CETOCOEN Excellence). This publication reflects only the authors' view, and

the European Commission is not responsible for any use that may be made of the information it contains.

## References

- 1 A. Hendy and D. Bakr, Indoor air quality between textiles' treatment and human health, *Int. J. Sci. Res.*, 2020, **9**, 200–206.
- 2 D. Won, R. L. Corsi and M. Rynes, New indoor carpet as an adsorptive reservoir for volatile organic compounds, *Environ. Sci. Technol.*, 2000, **34**, 4193–4198.
- 3 G. Morrison, N. V. Shakila and K. Parker, Accumulation of gas-phase methamphetamine on clothing, toy fabrics, and skin oil, *Indoor Air*, 2015, **25**, 405–414.
- 4 A. Saini, J. O. Okeme, J. Mark Parnis, R. H. McQueen and M. L. Diamond, From air to clothing: characterizing the accumulation of semi-volatile organic compounds to fabrics in indoor environments, *Indoor Air*, 2017, **27**, 631–641.
- 5 R. E. Noble, Environmental tobacco smoke uptake by clothing fabrics, *Sci. Total Environ.*, 2000, **262**, 1–3.
- 6 A. Saini, C. Thaysen, L. Jantunen, R. H. McQueen and M. L. Diamond, From clothing to laundry water: investigating the fate of phthalates, brominated flame retardants, and organophosphate esters, *Environ. Sci. Technol.*, 2016, **50**, 9289–9297.
- 7 J. J. Piadé, S. D'André and E. B. Sanders, Sorption phenomena of nicotine and ethenylpyridine vapors on different materials in a test chamber, *Environ. Sci. Technol.*, 1999, **33**, 2046–2052.
- 8 E. T. Borujeni, K. Yaghmaian, K. Naddafi, M. S. Hassanvand and M. Naderi, Identification and determination of the volatile organics of third-hand smoke from different cigarettes and clothing fabrics, *J. Environ. Health Sci. Eng.*, 2022, **20**, 53–63.
- 9 Y.-C. Chien, C.-P. Chang and Z.-Z. Liu, Volatile organics off-gassed among tobacco-exposed clothing fabrics, *J. Hazard. Mater.*, 2011, **193**, 139–148.
- 10 A. Saini, C. Rauert, M. J. Simpson, S. Harrad and M. L. Diamond, Characterizing the sorption of polybrominated diphenyl ethers (PBDEs) to cotton and polyester fabrics under controlled conditions, *Sci. Total Environ.*, 2016, **563–564**, 99–107.
- 11 D. Licina, G. C. Morrison, G. Bekö, C. J. Weschler and W. W. Nazaroff, Clothing-Mediated exposures to chemicals and particles, *Environ. Sci. Technol.*, 2019, **53**, 5559–5575.
- 12 L. Petrick, H. Destailats, I. Zouev, S. Sabach and Y. Dubowski, Sorption, desorption, and surface oxidative fate of nicotine, *Phys. Chem. Chem. Phys.*, 2010, **12**, 10356–10364.
- 13 E. D. Schreder and M. J. La Guardia, Flame Retardant Transfers from U.S. Households (dust and laundry wastewater) to the aquatic environment, *Environ. Sci. Technol.*, 2014, **48**, 11575–11583.
- 14 Ö. Edebalı, S. Krupčíková, A. Goellner, B. Vrana, M. Muz and L. Melymuk, Tracking aromatic amines from sources to surface waters, *Environ. Sci. Technol. Lett.*, 2024, **11**, 380–492.



- 15 D. M. DeMarini, T. Carreón-Valencia, W. M. Gwinn, N. B. Hopf, M. S. Sandy, T. Bahadori, G. M. Calaf, G. Chen, A. de Conti, L. Fritschi, M. Gi, P. D. Josephy, J. Kirkeleit, K. Kjaerheim, S. Langouët, D. M. McElvenny, C. M. Sergi, L. T. Stayner, T. Toyoda, Y. Grosse, L. Benbrahim-Tallaa, F. El Ghissassi, E. Suonio, M. C. Turner, I. A. Cree, H. Mattock, K. Müller, F. Chung, K. Z. Guyton and M. K. Schubauer-Berigan, Carcinogenicity of some aromatic amines and related compounds, *Lancet Oncol.*, 2020, **21**, 1017–1018.
- 16 T. Sugimura, K. Wakabayashi, H. Nakagama and M. Nagao, Heterocyclic amines: Mutagens/carcinogens produced during cooking of meat and fish, *Cancer Sci.*, 2004, **95**, 290–299.
- 17 P. Vineis and R. Pirastu, Aromatic amines and cancer, *Cancer, Causes Control, Pap. Symp.*, 1997, **8**, 346–355.
- 18 IARC, List of Classifications; Agents Classified by the IARC Monographs, <https://monographs.iarc.who.int/list-of-classifications>, (accessed May 3, 2024).
- 19 Z. Tian, M. Gonzalez, C. A. Rideout, H. N. Zhao, X. Hu, J. Wetzel, E. Mudrock, C. A. James, J. K. McIntyre and E. P. Kolodziej, 6PPD-Quinone: Revised toxicity assessment and quantification with a commercial standard, *Environ. Sci. Technol. Lett.*, 2022, **9**, 140–146.
- 20 Z. Tian, H. Zhao and P. Katherine T, A ubiquitous tire rubber-derived chemical induces acute mortality in coho salmon, *Science*, 2021, **371**, 185–189.
- 21 M. Muz, M. Krauss, S. Kutsarova, T. Schulze and W. Brack, Mutagenicity in surface waters: synergistic effects of carboline alkaloids and aromatic amines, *Environ. Sci. Technol.*, 2017, **51**, 1830–1839.
- 22 S. Chinthakindi and K. Kannan, Primary aromatic amines in indoor dust from 10 countries and associated human exposure, *Environ. Int.*, 2021, **157**, 106840.
- 23 US Environmental Protection Agency, *CompTox Chemicals Dashboard*|Home.Version v2.5.0, <https://comptox.epa.gov/dashboard/>, accessed November 15, 2024.
- 24 A. J. Williams, C. M. Grulke, J. Edwards, A. D. McEachran, K. Mansouri, N. C. Baker, G. Patlewicz, I. Shah, J. F. Wambaugh, R. S. Judson and A. M. Richard, The CompTox Chemistry Dashboard: a community data resource for environmental chemistry, *J. Cheminf.*, 2017, **9**, 61.
- 25 S. Grishanov, *Handbook of Textile and Industrial Dyeing: 2 - Structure and Properties of Textile Materials* Elsevier, 2011, pp. 28–63.
- 26 M. El Messiry, A. El Ouffy and M. Issa, Microcellulose particles for surface modification to enhance moisture management properties of polyester, and polyester/cotton blend fabrics, *Alexandria Eng. J.*, 2015, **54**, 127–140.
- 27 W. Tegegne and A. Haile, Improving hydrophilicity and comfort characteristics of polyester/cotton blend fabric through lipase enzyme treatment, *Clean Technol. Environ. Policy*, 2024, **27**, 3–16.
- 28 G. K. Pierens, T. K. Venkatachalam and D. Reutens, A comparative study between *para*-aminophenyl and *ortho*-aminophenyl benzothiazoles using NMR and DFT calculations, *Magn. Reson. Chem.*, 2014, **52**, 453–459.
- 29 G. C. Morrison, H. V. Andersen, L. Gunnarsen, D. Varol, E. Uhde and B. Kolarik, Partitioning of PCBs from air to clothing materials in a Danish apartment, *Indoor Air*, 2018, **28**, 188–197.
- 30 J. Yu, F. Wania and J. P. D. Abbatt, A New Approach to Characterizing the partitioning of volatile organic compounds to cotton fabric, *Environ. Sci. Technol.*, 2022, **56**, 3365–3374.
- 31 A. Eftekhari and G. C. Morrison, A high throughput method for measuring cloth-air equilibrium distribution ratios for SVOCs present in indoor environments, *Talanta*, 2018, **183**, 250–257.
- 32 G. Morrison, H. Li, S. Mishra and M. Buechlein, Airborne phthalate partitioning to cotton clothing, *Atmos. Environ.*, 2015, **115**, 149–152.
- 33 L. M. Petrick, A. Svidovsky and Y. Dubowski, Thirdhand Smoke: Heterogeneous oxidation of nicotine and secondary aerosol formation in the indoor environment, *Environ. Sci. Technol.*, 2011, **45**, 328–333.

